Research Square

Preprints are preliminary reports that have not undergone peer review.
They should not be considered conclusive, used to inform clinical practice,
or referenced by the media as validated information.

Developmental stage and hormonal signaling impact gut microbiome composition and functional potential in wild Rana sylvatica tadpoles

Samantha M. Tracy

samantha.tracy@yale.edu

Yale University

David K. Skelly

Yale University

Article

Keywords: Microbiome, Amphibians, Development, Hormones, Stress, Metamorphosis

Posted Date: November 24th, 2026

DOI: https://doi.org/10.21203/rs.3.rs-11391978/v1

License: This work is licensed under a Creative Commons Attribution 4.0 International License.
Read Full License

Additional Declarations: No competing interests reported.

Title: Developmental stage and hormonal signaling impact gut microbiome composition and functional potential in wild *Rana sylvatica* tadpoles

Authors: Samantha M. Tracy[1*] and David K. Skelly[1,2]

1. School of Environment, Yale University, New Haven, CT, United States
2. Peabody Museum, Yale University, New Haven, CT, United States

[*]**Corresponding Author Email:** samantha.tracy@yale.edu

Keywords: Microbiome, Amphibians, Development, Hormones, Stress, Metamorphosis

Abstract: Most amphibians undergo a complex, multi-stage life cycle that requires major shifts in diet, physiology, and endocrine signaling. The gut microbiome, with its varied composition and functional pathways, is influenced by both developmental changes and physiological signaling. In this study, we assessed changes in diversity, composition, and functional pathways of the gut microbiome during wood frog larval development. Additionally, we analyzed tissue corticosterone (CORT) concentrations to assess the relationship between glucocorticoid signaling, development, and microbiome composition. Tadpole gut contents and tissue samples were collected bi-weekly from twelve natural pond sites across two geographic locations in Connecticut to assess both microbiome changes and associated CORT signaling over development. Overall, we found a decrease in microbiome alpha-diversity during larval development despite pond-level variation. Models showed a sharp decline in alpha diversity during pre-metamorphosis, accompanied by substantial changes in taxonomic composition and shifts in functional pathways. We found decreases in microbiome diversity with increasing baseline CORT levels, accompanied by shifts in taxonomy and functional pathways, indicating potential links between endocrine system responses and microbial presence. CORT was also associated with increased abundance of pathogenic microbes. For amphibians, these findings further elucidate gut microbiome interactions with development, glucocorticoid signaling, and preparation for metamorphosis.

Introduction:

Habitat loss, coupled with a changing climate, is leading to major declines in amphibian populations.[1] Increased evidence throughout the animal kingdom has shown that the interplay between an organism's internal and external environment may be a key physiological mechanism for maintaining homeostasis and increasing survival[2]. In amphibians, the gut and skin microbiomes are both known to respond to and adapt to changing conditions, aiding growth, survival, and development.[3–5] The gut microbiome also plays a key role in metabolism and energy allocation throughout the developmental window. Microbiota form a symbiotic relationship with the host organism that affects digestion, energy transfer, development, and immune response.[4,6,7] The larval gut microbiome functions through co-evolutionary relationships between bacterial communities and a host, driven by diet-mediated selection.[8–10] During development, the intestinal tract of tadpoles shrinks in preparation for the metamorphic transition; this is coupled with concurrent shifts in the microbiome as tadpoles transition from herbivorous to primarily carnivorous diets.[11,12] Despite variations in environmental conditions, the strongest driver of variation in tadpole microbial composition is developmental stage, suggesting strong host and developmental factors govern microbiome shifts even in shifting

environments.[13] Disruption of the microbiome during critical developmental windows in pre-metamorphic tadpoles has been shown to affect long-term physiological performance, disease outcomes, and parasitic infection rates.[14,15] Conversely, disruptions of standard growth and development by disease also result in microbiome composition changes.[16]

In response to changing conditions, amphibians have demonstrated rapid plastic responses that improve survival[17]. Tadpoles can directly respond to changes in their environment through mechanisms of developmental plasticity, adjusting their developmental rate in response to favorable or unfavorable environmental conditions for growth and survival[17,18]. Plastic responses rely heavily on endocrine pathways, and in tadpoles corticosterone (CORT) is the primary effector hormone modulating physiological and behavioral responses to environmental stimuli. CORT is commonly cited as the "stress" hormone, governing the hypothalamic-pituitary-interrenal (HPI) axis and associated downstream responses.[18] Throughout development, energy balance must occur to ensure adequate resource direction towards environmental response (i.e., predator avoidance and thermal adjustment), while maintaining enough energy stores to promote growth and development. This energy balance is also regulated via the endocrine system, with CORT modulating metabolic responses. CORT signaling may shift energy allocation and accelerate development while sacrificing growth in particularly stressful or drying environments.[19] Despite the necessity of endocrine pathway modulation for plastic responses, long-term increased activation of CORT is known to have other harmful physiological effects, primarily decreased immune function and changes in gut microbial diversity and abundance.[20] Prolonged stress exposure or continual stress activation can have detrimental effects on microbiome properties, posing potential issues with long-term health and microbial colonization as tadpoles reach metamorphic transition[7,21].

While the physiological underpinnings of developmental plasticity are linked to hormonal mechanisms, there has been little documentation of how the gut microbiome may respond or work in tandem with the endocrine system throughout development.[22,23] Assessing shifts in microbiome diversity and abundance across the developmental window, while simultaneously investigating patterns of CORT production, allows us to gain a higher-level understanding of synergistic mechanisms and physiological shifts that occur during tadpole development. The potential interactions among gut microbiome health, CORT production, and conservation efforts remain largely unexplored. However, current research suggests interactions that may be a key facet of understanding plastic developmental responses to environmental changes.[3,18–20]

In this study, we assessed the relationships among gut microbiome composition, larval development, and tissue CORT levels across several ponds at multiple time points in *Rana sylvatica* larvae (Figure 1). We had three primary objectives: (1) to assess shifts in microbiome diversity and composition throughout larval development; (2) to explore the interactive effects of gut microbiome composition and endocrine response using measurements of baseline corticosterone; and (3) to assess taxonomic and functional pathway shifts linked to both development and CORT secretion. Subsequently, microbiome patterns were quantified over a developmental time series across a set of natural ponds to assess these objectives in a relevant ecological context. Characterizing these microbiome transitions during development provides additional baseline data for further assessments of potential environmental drivers of gut dysbiosis. Identifying the stage-relevant properties of the gut microbiome is critical baseline data

to evaluate as we continue to explore drivers of amphibian decline and understand the symbiotic relationships between amphibians and their host microbiomes. Further assessment of the interactions between baseline CORT and microbiome dynamics is important for understanding how shifts in endocrine pathways and plastic mechanisms may interact with the gut microbiome.

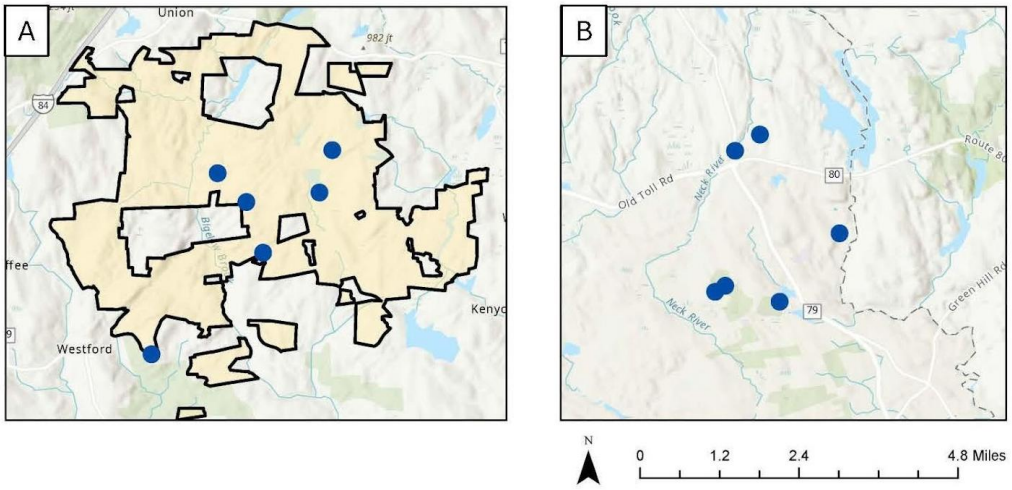

Figure 1: Map of study ponds in CT A) Ponds in the Yale Myers Forest with Forest property boundary B) Ponds in Madison, CT

Results

Read Summary

We evaluated sequences from 200 samples (194 gut samples and 6 controls). Following library preparation, sequencing, quality filtering, merging, decontamination, and abundance and prevalence filtering, unrarefied data had a total of 79,706,690 reads (mean reads per sample = 410,859 ± 137,356 SD) from 194 gut samples.[27] This represented 32 phyla, 67 classes, 139 orders, 230 families, and 638 genera, with most reads belonging to the most abundant phyla: Bacillota (Firmicutes), Pseudomonadota (Proteobacteria), Actinomycetota, and Bacteroidota (Supplementary Figure 1).

Relationships Between Alpha Diversity Metrics and Developmental Stage

There was a significant relationship between developmental stage and all three alpha diversity metrics (Supplementary Table S1, Figure 2). In all GAMs, stage was a significant predictor of alpha diversity (all $p < 0.001$; Supplementary Table S1). Larval pond was also a significant predictor of alpha diversity metrics and was controlled for in all models as a random effect (all $p \leq 0.009$). When averaged across the time series, diversity metrics varied among ponds (Supplementary Figure S2). For all metrics, alpha diversity showed a sharp decline after stage 38, corresponding to the onset of the metamorphic transition.

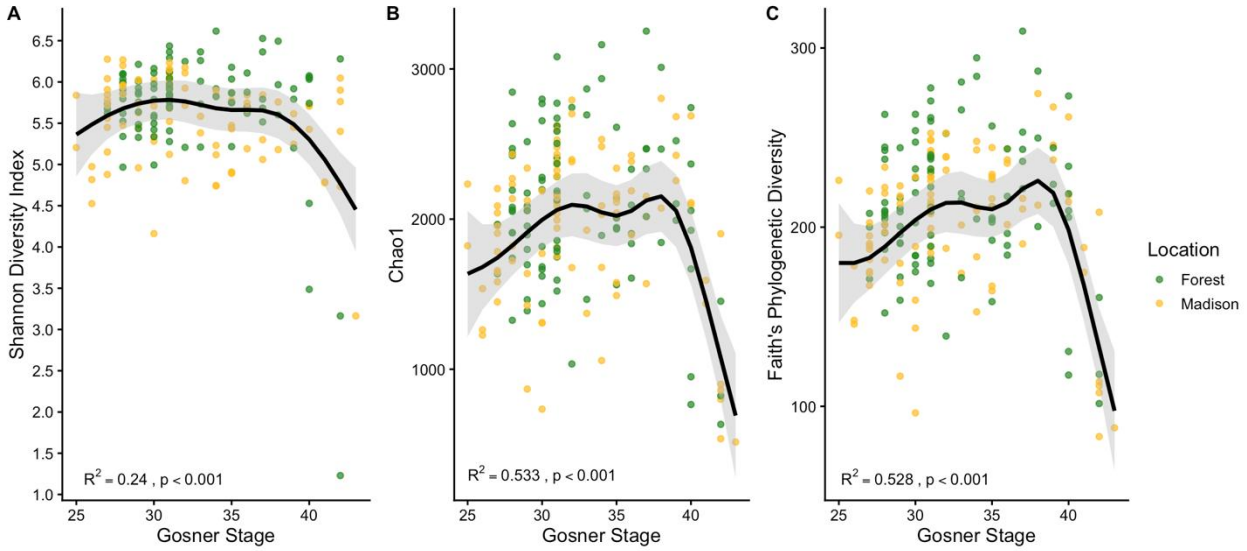

Figure 2: Changes in alpha diversity metrics across the developmental window (A) Shannon Diversity Index (R^2= 0.240, $p < 0.001$) (B) Chao1 (R^2= 0.533, $p < 0.001$) (C) Faith's Phylogenetic Diversity (R^2= 0.528, $p < 0.001$). Trend lines and confidence intervals were generated by predicting alpha metrics using the stage term in the model. The p-value represents the p-value of the smoothed stage term in the GAM.

Shifts in Microbiome Composition during larval development

After ordinating the distance matrices using PCoA methods we noted the variance explained by the first 5 axes (Supplementary Table S2, Figure 3), prior to conducting significance testing. The test for homogeneity of dispersion was not significant for any of the distance metrics, indicating that groups have equal variances for further statistical analysis, and a PERMANOVA will accurately show differences in group centroids (Bray: F = 0.82, p = 0.47, Unifrac: F = 1.41, p = 0.26, Weighted Unifrac: F = 2.05, p = 0.10). PERMANOVA tests using Bray-Curtis dissimilarities showed significant differences in microbiome composition between categorical stage groups (F = 6.26, p = 0.001), with post hoc pairwise comparisons indicating significant differences among all four categorical stage groups (BH-adjusted $p \leq 0.002$). Unweighted UniFrac distances also showed significant differences in microbiome composition between categorical stage groups (F = 3.86, p = 0.001), with post hoc pairwise comparisons indicating significant differences among all four categorical stage groups (BH-adjusted $p < 0.004$). Weighted UniFrac distances also showed significant differences in microbiome composition between categorical stage groups (F = 5.38, p =0.001), with post hoc pairwise comparison tests showing significant differences between all categorical stage groups (BH-adjusted $p \leq 0.008$), except for "Toe Differentiation" vs "Pre-Metamorphic" (BH-adjusted p = 0.145).

We also created a core microbiota Venn diagram to visualize differences in Amplicon Sequence Variants (ASVs) across the developmental window and to identify core microbiome ASVs present across stages. We defined the "core" as ASVs that were present in at least 70% of samples. We identified 116 core ASVs (17%). We observed notable shifts throughout the developmental window, with limb-development individuals having a unique set of 64 ASVs (10%) and pre-metamorphic individuals having a unique set of 69 ASVs (10%) (Figure 4A). To

examine changes in composition over a linear time series, we created a stacked bar chart representing the "average" composition by Order for an individual at each Gosner stage (Figure 4B).

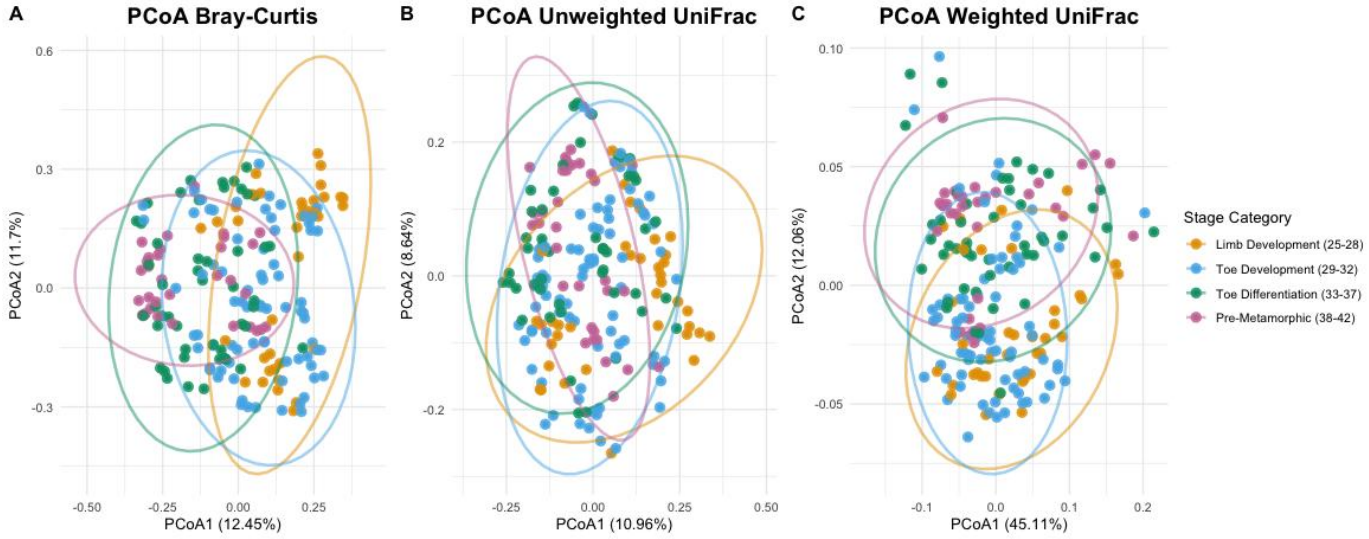

Figure 3: PCoA of three distance matrices clustered by stage category (A) Bray-Curtis ($F = 6.26$, $p = 0.001$) (B) Unweighted UniFrac ($F = 3.86$, $p = 0.001$) (C) Weighted UniFrac ($F = 5.38$, $p = 0.001$). Axes represent the first two principal components of PCoA analysis with the amount of variation explained noted in parenthesis.

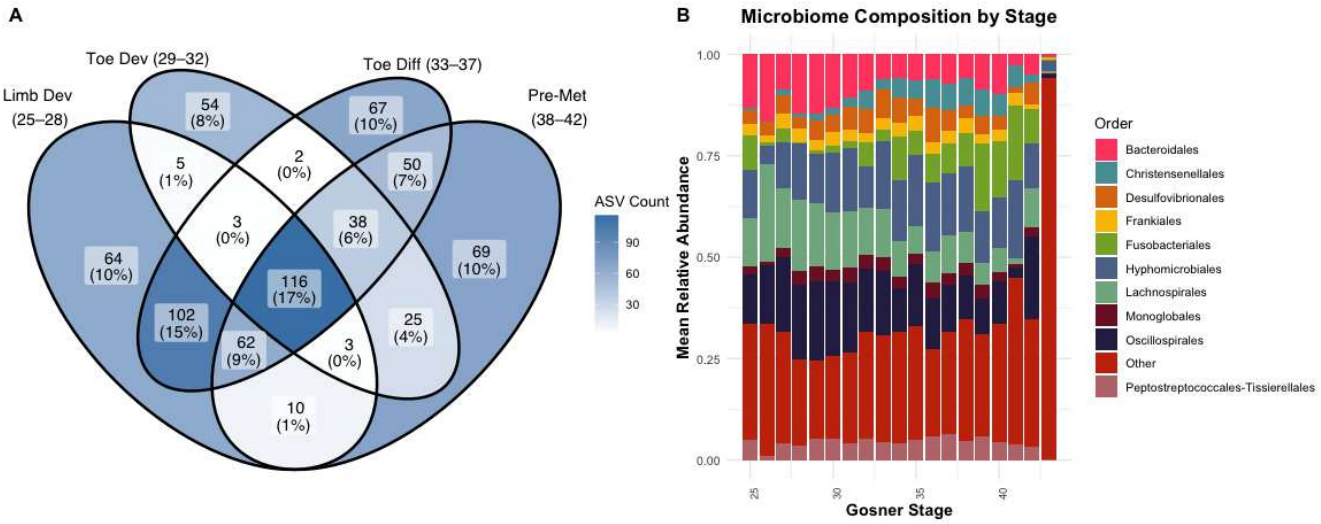

Figure 4: Shifts in the microbiome during development based on ASVs and Order. (A) Venn Diagram showing overlapping ASVs between various developmental stage categories. Circles correspond to distinct stage groupings; shading is consistent with the number of unique ASVs overlapping between circles and is consistent with the number and percent of total ASVs indicated inside the circle. (B) Stacked bar chart showing average relative abundance of Orders across Gosner stages

Relationships Between CORT & Microbiome Alpha Diversity

There was a relationship between average baseline CORT and some alpha diversity metrics (Supplementary Table S3, Figure 5). Stage was found to be a negative predictor of alpha diversity, as shown above, and was found to be a negative predictor of baseline CORT concentration in GEE models (ß = -0.033 ± , p = 0.012), so stage was included as a fixed effect in the models looking at the association of CORT and diversity metrics. Stage and CORT were evaluated for collinearity using variance inflation factors (VIFs) and were not found to be collinear for alpha diversity models (VIF > 5). Average baseline CORT was found to have a negative relationship with average Chao1 (ß = -235.8 ± 79.9, p = 0.003) and with average Faith's PD (ß = -18.27 ± 8.42, p = 0.03). However, a decreasing trend that failed to reach significance was observed between CORT and the average Shannon Diversity Index (ß = -0.138 ± 0.097, p = 0.153).

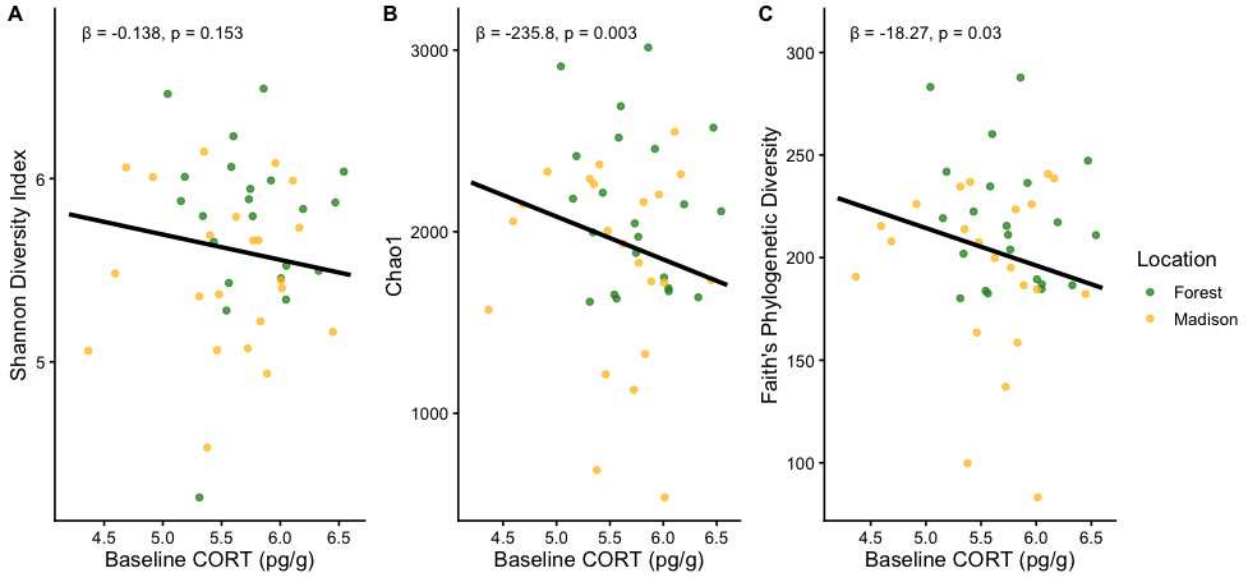

Figure 5: Modeled relationships between average natural log baseline CORT and alpha diversity metrics (A) Shannon Diversity Index (ß = -0.138 ± 0.097, *p* = 0.153) (B) Chao1 (ß = -235.8 ± 79.9, *p* = 0.003) (C) Faith's Phylogenetic Diversity (ß = -18.27 ± 8.42 *p* = 0.03). Trend lines were generated by predicting alpha metrics using the average baseline CORT term in the model. Beta values represent the beta coefficients of the CORT term in the GEE model and p-values are also specific to those model terms.

Associations of microbial genera and functional pathways with CORT & Development

Using negative binomial linear regression models to assess the relationship between stage and the abundance of gut microbial genera, while controlling for the random effect of larval pond, we identified 80 genera positively associated with stage and 94 negatively associated (Supplementary Table S5, Figure 6). Additional models assessing the relationship with average baseline CORT identified 12 genera positively associated with baseline CORT and 30 genera negatively associated (Supplementary Table S6, Figure 6). Additionally, we assessed associations between stage and CORT and gene enrichment, as described by KEGG. We found 4 positively associated descriptive gene sets with developmental stage and 11 negatively

associated (BH-adjusted $p < 0.05$) (Supplementary Table S7, Figure 7). We also found 15 positively associated descriptive gene sets with baseline CORT after controlling for developmental stage, and 28 negatively associated (BH-adjusted $p < 0.05$) (Supplementary Table S8, Figure 7).

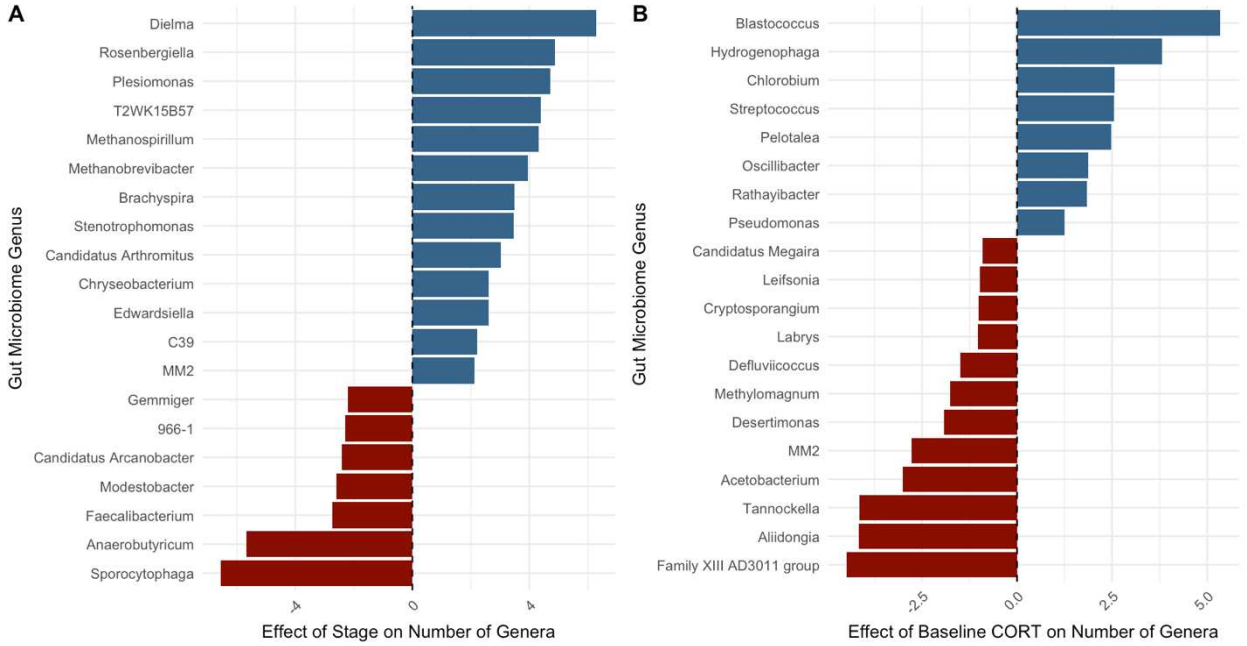

Figure 6: Effect estimates from negative binomial models showing the top 20 microbial genera associated with (A) developmental stage (BH adjusted p-value < 0.05) and (B) average baseline CORT when adjusting for stage (BH adjusted p-value < 0.05) . The x-axis shows modeled effect estimate sizes, the y-axis shows the names of microbial genera groups, the color shows the directionality of the effect estimate with blue bars indicating a positive association and red bars indicating a negative association.

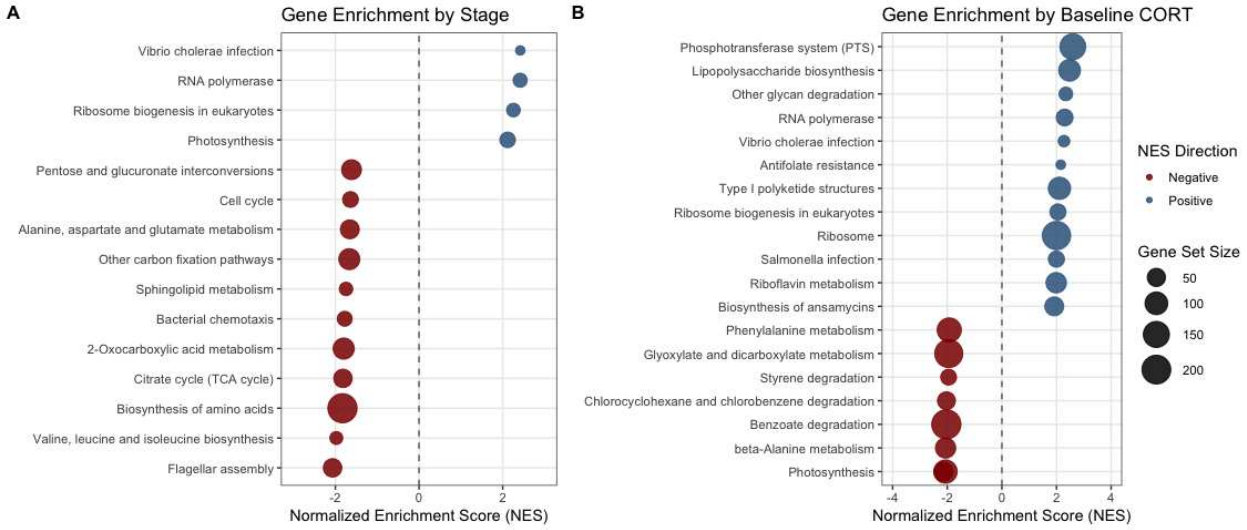

Figure 7: Top NES estimates of functional KEGG Pathways associated with (A) developmental stage and (B) Baseline CORT (Top 20 by NES). Normalized Enrichment Score is shown on the x-axis, and the direction of association is color coded with negative associations with stage shown in red and positive associations shown in blue. The number of genes associated in that descriptive category are depicted by the size of the symbol.

Discussion

Wood frog metamorphosis is a complex biological process in which nearly all physiological functions undergo profound changes as individuals transform from water-breathing aquatic omnivores to air-breathing terrestrial carnivores.[28] The cardiovascular system, digestive system, vision, and auditory systems each change to support the transition to a new environment and way of life. In Xenopus, metamorphosis results in a 75% shorter intestine and decreased microbiome diversity.[29] Other studies in a variety of amphibians have found decreased gut microbiome diversity when comparing tadpoles to post-metamorphic juvenile frogs.[11,28,30,31] Our study confirms these prior findings, showing that the physical metamorphic transition is associated with changes in gut microbial diversity and composition, with decreases in microbial diversity observed during the later stages of larval development. All indices showed a sharp decline in alpha diversity metrics after stage 38, corresponding to the pre-metamorphic stages and the preparation for terrestrial life. This decrease was accompanied by compositional changes in the gut microbiome, with notable shifts in beta diversity and various microbial ASVs across different stage categories. Many other studies have found differences in microbiome diversity and composition during the metamorphic transition, but our study is the first we are aware of to categorize changes beginning early in larval development (from stage 25) to metamorphic stages; however, it is not the first to categorize gut microbiome diversity across amphibian life stages.[13,31]

Past studies have found conflicting evidence regarding the directionality of the relationship between microbiome alpha diversity and "stress" hormone measures. A similar study in *Bufo bufo* tadpoles showed a significant positive association between CORT levels and alpha diversity metrics, the opposite of our findings.[24] While there is limited basis for understanding the difference in these relationships observed in different studies with different species, we know that responses are highly variable and likely driven by multiple factors. Our two studies also used different methods to assess gut microbiome diversity: ours sequenced the V3-V4 region, while the other used only the V4 region, both of which are common methods for assessing microbial diversity using 16S rRNA sequencing. Gabor et al. (2022) also used water-based CORT assays to measure hormonal levels non-invasively, whereas we used tissue CORT.

Other studies have also found negative relationships between CORT and alpha diversity. A study examining the amphibian skin microbiome in translocated treefrogs confirmed our findings in the skin microbiome, showing decreased diversity as cortisol levels increased.[3] Oral microbiome diversity was found to be lower with increased fecal glucocorticoid metabolites in wild red squirrels.[32] A separate study in wild red squirrels showed a significant negative relationship between measured glucocorticoids and three alpha diversity metrics.[21] In lizards, complex interactions were observed, with both CORT levels and gut microbiome diversity metrics showing strong dependence on gestational status and stage, further exemplifying how complex

biological and metabolic factors may influence the relationships between CORT and the gut microbiome.[33] In experimental studies, stress treatments have been shown to influence the diversity and composition of the gut microbiome in tadpoles as well as in primate species.[5,34] Diet-induced changes in microbiota may also mediate stress responses in larval amphibians, acting as a protective stress mechanism.[4]

When evaluating compositions changes in the gut microbiome, genera exhibiting the largest positive effect sizes associated with developmental stage included two methanogenic genera, *Methanospirillum* and *Methanobrevibacter*. *Rosenbergiella* was also positively associated with stage; this taxon is thought to have beneficial immune functions and has been shown to disrupt virus colonization in mosquitoes.[35] While the functionality of changes in genera abundance with stage is still unknown, the increase and decrease of certain genera confirms the additional evidence of community composition changes as tadpoles reach metamorphosis. Genera exhibiting strong negative associations: *Anaerobutyricum*, a butyrate-producing genus, and *Sporocytophaga*, a cellulose-degrading genus primarily isolated from soils,[36] could indicate taxonomic shifts linked with changes in diet and digestive system function[28,37]. When controlling for stage, genera showing strong associations with baseline CORT included *Blastococcus*, *Streptococcus,* and *Family XII AD3011group*. Increased abundance of *Streptococcus* has been linked to inflammation and chronic disease in human populations, and is known to be an opportunistic pathogen.[38] As CORT is involved in both metabolic and inflammatory responses, this further suggests a link between upregulated baseline CORT and a potential increase in pathogen presence. *Family XII AD3011* has been noted as a beneficial microbial group that inhibits inflammation[39]; a decrease in the *Family XII AD3011* group was observed with increasing baseline CORT values, suggesting a potential link between increased glucocorticoid production and changes in the microbiota that provide anti-inflammatory functionality.

Functional analysis of the microbiome revealed similar patterns in community composition shifts, with functional patterns shifting with both developmental stage and baseline CORT concentration. Developmental stage was positively associated with functional capacities for transcription and translation, as well as energy metabolism and bacterial infectious disease. In contrast, carbohydrate, amino acid, and lipid metabolism were all negatively associated with development. Functional enrichment of glycan biosynthesis, membrane transport, vitamin metabolism, and bacterial infectious disease was all positively associated with baseline CORT. Terpenoid and polyketide, amino acid, carbohydrate and xenobiotic metabolism were all negatively associated with baseline CORT. Functional shifts in the microbiome have previously been noted when comparing tadpoles, froglets, and adult frogs, with metabolic pathways and aerobic respiration decreasing in froglets and adult frogs compared to tadpoles, suggesting changes in metabolic needs through development.[37]. These functional groupings further underscore the complex response and the interactive effects of CORT, development, metabolism, and gut microbial health, as short-term higher levels of CORT may be useful in promoting development, plasticity, and response,[40,41] but long-term high baseline levels may lead to negative functional changes in metabolic profile, immunity, and downstream interactions with gut microbes.

Continued research is warranted to elucidate how signaling factors are interconnected and to establish the potential for a bidirectional gut-endocrine axis in developing amphibians. Past

studies have attempted to understand the directionality and negative feedback system of endocrine signaling and microbiome response.[5,24,42] Future studies should continue to explore the drivers of gut microbiome variation in natural amphibian populations and consider how life stages impact observed patterns in microbial composition. Further investigation into the roles of symbiotic microbes in amphibian physiology is needed as we continue to employ management strategies to combat ongoing population declines. Our findings are relevant to understanding the drivers and physiological shifts associated with the environmental stress response and aim to provide baseline information on microbiome composition and interactions with development and endocrine physiology to assist with large-scale amphibian conservation efforts.

Methods

Study Sites & Species:

The Yale Myers Forest (YMF) is a 3,213-hectare property owned by Yale University, located in Northeastern Connecticut between the towns of Union, Ashford, and Westford. For this study, twelve ponds were selected for sample collection. Ponds were split evenly between the Yale Myers Forest (YMF), a 3,213-hectare property owned by Yale University located in Northeastern Connecticut between the towns of Union, Ashford, and Westford, and Madison, CT, a suburban coastal town in New Haven County with approximately 18,000 residents. Ponds were selected to represent varying vernal pond conditions, including hydroperiod, area, canopy cover, proximity to urban spaces, and water quality across the two geographic locations. Sample locations are shown in Figure 1. In this study, we targeted *Rana sylvatica* tadpoles known to inhabit these pond sites. *Rana sylvatica* is a widespread North American amphibian known for explosive breeding, primarily laying eggs in fishless, temporary vernal ponds. Tadpoles normally fully develop from eggs to metamorphs within 60 to 90 days, but development is highly dependent on genetics, environmental, and pond condition.[43,44]

Sample Collection:

Samples were collected from pond sites every two weeks between May 12, 2025, and July 11, 2025. At each visit, 10 tadpoles were collected during timed dip netting. The amount of time spent sampling each pond was based on area, water level, and ease of movement in the pond, allowing enough time to cover the entire surface area without repeat sampling. Collected tadpoles were subjected to a stress assay to determine both baseline and stressor-induced tissue CORT concentrations (detailed below). Additionally, water quality measurements were collected at predetermined, marked locations near the entry basin of each pond. Water quality metrics, including temperature, pH, total dissolved solids (TDS), conductivity, and salinity, were measured using an Oakton PCTESTr 50 5-in-1 multimeter. Nitrate levels were collected using a LAQUAtwin NO_3^- meter.

Tadpole Collection & Novel Stressor Hormonal Response Assay

The stress assay was adapted from Gabor et al., 2013.48 All stress assays were performed immediately after tadpole collection, while still at the pond site, using aged, aerated well water. After collection, all tadpoles were placed in individual 120 mL cups filled with 100 mL of water for 1 hour to establish a baseline. After one hour, five of the collected tadpoles were immediately euthanized, placed in individually labeled tubes, and placed on ice. The remaining five tadpoles were moved to a second 120 mL cup filled with 100 mL of water and gently agitated by cup-swirling every 3 minutes for one hour to induce a novel stress response and provoke secretion of

tissue corticosterone. After one hour, tadpoles were immediately euthanized with a 10% ethanol solution, resulting in full euthanasia in two to four seconds observed by cessation of movement.[45] As euthanasia was quick and completed at the field site no anesthetic was utilized. Tadpole samples were immediately placed in labeled 5mL tubes on ice. After field collection, all tissue samples were immediately taken to the lab, flash-frozen by submersion in dry ice, and stored at -80 ºC until hormone analysis. Prior to hormone analysis, all samples were measured for snout-vent length (SVL) and assigned a Gosner stage.[46] In this study, only baseline tissue CORT values were used. Stress induced tissue samples were used for another project. All protocols involving tadpoles were approved by Yale's IACUC protocol # 2025-10361. Tadpoles were collected under CT Department of Energy & Environmental Protection permit #2528001 with field survey permission from the Yale Myers Research Committee (TRA24). All methods including collection, assay, and euthanasia were performed in accordance with the relevant guidelines and regulations as indicated by the above protocols, permits, and the Guidelines for Use of Live Amphibians and Reptiles in Field and Laboratory Research.

Hormone Analysis

For CORT analysis, tadpoles were defrosted, dissected to remove the intestinal tract, and bisected at the start of the tail. For baseline samples, the intestinal tract of each tadpole was stored at -80 ºC after dissection until microbiome analysis. In most instances, these were the same individuals sampled for tissue CORT levels, in cases where tissue CORT could not be obtains (i.e. failed extraction, or high CV value between replicates) a replacement individual from the same pond at the same timepoint was used for CORT analysis. Hormones were then extracted from tissue samples using a modified diethyl ether and petroleum ether protocol from Gomez-Mestre et al., 2013.[47] The body cavity tissue was weighed, then homogenized in 0.5mL of PBS buffer using a Kinematica Polytron PT 2500E Homogenizer (Kinematica Global, Bohemia, NY) at top speed for 10 seconds. A 70% diethyl ether-30% petroleum ether mixture was then added to each sample in 4mL quantities. Samples were centrifuged at 1800 RPM at 5 °C for 15 minutes and flash-frozen using a mixture of dry ice and ethanol to separate steroid hormone compounds. The liquid phases of each sample were decanted, an additional 4mL of solvent was added to each sample, and the centrifugation, flash freezing, and decanting procedures were repeated to ensure maximum CORT recovery. Ether was then evaporated using a WYDDDARY 24 Place Dry Nitrogen Blower with constant nitrogen flow (WYDDDARY, Yantai, Shandong, China). Dried down lipids were then resuspended in 400 µL of assay buffer. Samples were incubated overnight at 4 ºC and vortexed prior to analysis.

Extracted samples were then analyzed for CORT tissue concentrations using Arbor Assay Multiformat CORT Kits (Catalog Number K014-H1/H5). Samples were run in duplicate using the kit's 50 µL format according to the manufacturer's instructions, with relevant standard curves and controls, and read at a wavelength of 450nm using an Agilent BioTek 800TS Plate Reader (Agilent Technologies, Santa Clara, CA). Standard curves were generated using Gen5 software, and sample concentrations were determined from absorbance, the standard curve, and negative controls. Each plate contained a negative control and both high- and low-CORT solutions with known values to serve as positive controls. In total, 18 plates containing 421 samples were run, with an average R2 value for 4PLC curves of 99.7%, an average intra-assay variation of 15.6%, and an average inter-assay variation of 9.61%. Samples with a CV > 30% or plates with inaccurate standard curves were rerun or excluded from the dataset; any sample with a value

below 26.2 pg/µL was also removed from the dataset, as this is below the published sensitivity limit for the 50 µL format of the Arbor Assay kit. Hormone concentration was adjusted for extraction tissue weight and reconstitution volume and is expressed in picograms of corticosterone per gram of extracted tissue (pg/g) (n = 339 total samples, 169 baseline and 170 stressed). Multiple serial dilutions of pooled extracted sample product were tested at 1:1, 1:2, 1:4, and 1:8 concentrations to ensure parallelism with the standard curve and accurate EIA readings. Parallelism was demonstrated across all tested pooled samples, indicating that the EIA accurately measured CORT concentrations in the extracted samples.

All CORT values were natural-log-transformed to normalize the data. Since individual-level hormone data exhibit high variation and there is likely a time delay in how endocrine function may impact microbial diversity, we chose to average CORT concentrations per pond per timepoint (n = 44) and aggregate these with matching microbiome data for each pond at each timepoint. This method eliminates potential outliers in both baseline CORT and microbial diversity, allowing us to see effects at the pond level, where variation in both variables is likely to be most meaningful. Averaged CORT concentrations were used for modeling relationships between CORT and microbiome diversity, assessing potential CORT induced changes in Genera dynamics, and assessing functional pathway outcomes.

Microbiome Sample Processing

To assess microbiome diversity, five individual tadpole microbiome profiles from the baseline condition were used for each pond at each sample time point. Prior to DNA extraction, intestinal tract samples were thawed to room temperature. DNA extractions were performed using the QIAGEN DNeasy PowerSoil Pro Kit and following QIAGEN protocols, yielding 100 µL of extracted DNA. Three additional extraction blank controls were run to assess for contamination. Extracted DNA was stored at -20ºC. A 25 µL subset of the extracted DNA from each sample was transferred into a labeled 96-well plate, placed in a plastic bag, packed on dry ice, and shipped overnight to the University of Minnesota Genomics Center (UMGC) in Minneapolis, MN. Upon reaching UMGC, the sample DNA quantity was determined using 1:8 and 1:64 dilutions, and the sample was subjected to qPCR using primers V3_357F_Nextera (CCTACGGGAGGCAGCAG) and V4_806R_Nextera (GACTACHVGGGTATCTAATCC) targeting the V3-V4 locus in the 16S rRNA gene. Based on the output, samples were then diluted with water to normalize concentrations. Amplicons were generated by performing 25-cycle PCRs on the sample DNA using the same primer pair. PCR products were then diluted 1:100 in water and subjected to a second 10-cycle PCR to attach Illumina sequencing primer-compatible DNA regions and individual sample barcodes. Samples were all uniquely dual-indexed, as detailed in Gohl et al.[48] Final PCR products were normalized using the Just-a-Plate DNA Normalization kit (Charm Biotech, Cape Girardeau, MO), pooled into a sequencing library, and cleaned with AMPure XP mag beads (Beckman Coulter). Final amplicon size was confirmed by testing an aliquot of final library with an Agilent D1000 TapeStation instrument (Agilent Technologies, Santa Clara, CA). An aliquot of the final sequencing library was loaded onto an Element AVITI instrument using a 2x300 Medium Run flow cell (Element Biosciences, San Diego, CA) for sequencing. Sequenced samples included gut samples, extraction controls, and sequencing controls (n=200, 194 gut samples, 6 controls).

Microbiome Sequencing Analysis

Prior to processing, raw files were checked using FastOCv0.12.1 to ensure high-quality reads.[48,49] Files were then processed using *cutadapt* in R to trim adapters and primers.[50] The DADA2 package in R was used to filter low-quality reads, dereplicate sequences, calculate error rates, and merge sequences to create individual sample sequence data for taxonomic analysis.[51] Forward reads were filtered and trimmed to 280 base pairs, while reverse reads were filtered and trimmed to 220 to ensure complete merging for the V3-V4 target region. The default settings in the DADA2 pipeline were used for learning error rate, dereplication, and chimera removal. Taxonomy was assigned to each ASV sequence using a Naïve Bayes classifier trained with the Silva SSU Version 138.2.[52] After ASV assignment, any remaining chloroplast and mitochondrial sequences were filtered out. Extraction blank contamination was removed using the decontam package.[53] To remove ultra-rare and likely erroneous ASVs, a phylogenetic tree was built using only ASVs with at least ten reads using *MAFFT* [54] and *VeryFasTree*[55]. To standardize sequencing depths, all samples were rarefied to 10,000 sequences per sample. None of the three extraction blanks met the threshold and were removed from the dataset prior to downstream analysis. All other sequencing controls were removed prior to alpha- or beta-diversity analyses (n = 194). Rarefied data were used for alpha diversity and taxonomic metrics to remove any bias in diversity calculations or abundance metrics resulting from differing sequencing depths. Non-rarefied data were used for all other beta diversity and compositional analyses. A summary of all processed reads, including raw counts, trimming, filtering, merging, and chimera removal, is shown in Supplementary Table S4.

Statistical Analysis

All analysis was performed in R version 4.5.2.

Modeling Relationships Between Alpha Diversity Metrics and Developmental Stage

To assess the relationship between alpha diversity and developmental stage, we used generalized additive models (GAMs) with restricted maximum likelihood estimation in the *mgcv* package.[56] Alpha diversity metrics were calculated using the *microbiome* package.[57] We modeled relationships with stages for three metrics of alpha diversity: Shannon Diversity Index to account for both richness and evenness, Chao1 to assess species richness, and Faith's Phylogenetic Diversity to assess feature diversity. For Faith's Phylogenetic Diversity, the phylogenetic tree was rooted at the midpoint using the *phangorn* package[58] and metrics were calculated using the *picante* package.[59] Gosner Stage was used to categorize developmental stages numerically, values ranging from 25 to 43 and (n=194). Stage was included as a fixed smooth effect, and sample pond was included as a smooth random intercept. For GAMs, we selected a k value of 10 to avoid both overfitting and constraining the model and found that our effective degrees of freedom were well below k; our k index was 1, with p-values ranging from 0.38 to 0.86.

Computing the Shifts in Microbial Composition Across the Developmental Window

To explore how microbiome composition and relative taxon abundance shift over the developmental window, we computed distance matrices using the Bray-Curtis, UniFrac, and weighted UniFrac methods. Distance matrices were then used to compute PCoA and determine the variance explained by the first 5 PCoA axes. These distance matrices were used for all categorical grouping calculations to assess differences across groups. For the different

categorical stage groupings, there were 37 individuals represented in "Limb Development" stages 25 to 28, 32 individual tadpoles in "Toe Development" stages 29-32, 77 tadpole samples in "Toe Differentiation" stages 33-37, and 47 in the "Pre-Metamorphic" group- stages 38-42. Compositional shifts were examined using principal coordinates analysis (PCoA). We used three distinct distance methods – Bray-Curtis, weighted UniFrac, and unweighted UniFrac using the *vegan* package.[60] To determine how species vary proportionally across samples, data were transformed using the Hellinger method[61]. For weighted and unweighted UniFrac we used a phylogenetic tree rooted at the midpoint using the *phyloseq* package. We first used PCoA to assess the variation explained by categorical changes in developmental stage. We then assessed the homogeneity of dispersion for each distance metric to ensure that subsequent between-group comparisons could detect meaningful differences. To assess between-group differences, we then used PERMANOVA analysis with 999 permutations and post hoc pairwise comparisons with 999 permutations using the *pairwiseAdonis*[62] and *vegan* package. All p-values were adjusted using the Benjamini-Hochberg (BH) method to control the false discovery rate in multiple comparisons.

Estimating Relationships Between Alpha Diversity Metrics and CORT

To determine potential relationships between alpha diversity metrics of the gut microbiome and CORT secretion across the developmental window, we used generalized estimating equation (GEE) models in the *geepack* package.[63] GEE models allowed us to analyze population-averaged effects using an autoregressive order-1 correlation structure to account for repeated measures over time at the same pond sites.[24] As stage is known to have a significant effect on both microbial diversity and CORT production[13,64,65], we included stage as a variable in the models to assess the relationship between baseline CORT and the three metrics of alpha diversity described above (Shannon Index, Chao1, Faith's PD).

Taxonomic Shifts with CORT and Development

To investigate relationships between microbial genus abundance, baseline CORT, and developmental stage, we used negative binomial generalized linear models (nbGLM) with the *glmmTMB* package.[66] Models were run to regress the effects of stage, with sample pond as a random effect, on genus-level microbial abundance. Since non-rarefied data were used, we also controlled for log-transformed sequencing depth to minimize trends due to sequencing variation. Secondary models were run to assess the effects of adding pond-timepoint averaged baseline CORT on bacterial abundance dynamics. Both CORT and stage were scaled so effect sizes would be easily interpretable across models. All corresponding modeled p-values were corrected using the BH adjustment to identify significant positive or negative relationships between variables and microbial abundance.

Functional Shifts with CORT and Development

Using the *PICRUSt2* pipeline, functional components of bacterial communities were predicted from each sample[67]. *PICRUSt2* was used with default settings to generate metagenome predictions for each sample and subsequently to predict Kyoto Encyclopedia of Genes and Genomes (KEGG)[68,69] orthology abundances. Pearson correlations between KEGG Ortholog (KO) abundances and stage were computed and ranked. Using a linear model with regressed baseline CORT with stage to compute residual baseline CORT to identify CORT variation not explained by stage and providing a stage-adjusted CORT value. This adjusted CORT was then

used to compute Pearson correlations with KO abundances and ranked. We then used gene set enrichment analysis on KEGG pathways to assign and visualize predicted functional components correlated with developmental stage and residual baseline CORT using the package *clusterProfiler*.[70]

References:

1. Luedtke, J. A. *et al.* Ongoing declines for the world's amphibians in the face of emerging threats. *Nature* **622**, 308–314 (2023).
2. Karaer, M. C., Čebulj-Kadunc, N. & Snoj, T. Stress in wildlife: comparison of the stress response among domestic, captive, and free-ranging animals. *Front. Vet. Sci.* **10**, 1167016 (2023).
3. Neely, W. J. *et al.* Linking microbiome and stress hormone responses in wild tropical treefrogs across continuous and fragmented forests. *Commun Biol* **6**, 1261 (2023).
4. Hughey, M. C. *et al.* Diet- and salinity-induced modifications of the gut microbiota are associated with differential physiological responses to ranavirus infection in *Rana sylvatica*. *Phil. Trans. R. Soc. B* **378**, 20220121 (2023).
5. Emerson, K. J., Shaikh, S. S., Bradley-Slagle, D. P. & Woodley, S. K. The Aquatic Microbial Environment Shapes the Tadpole Microbiome and Antipredator Behavior. *Integrative And Comparative Biology* **65**, 783–795 (2025).
6. Frankiensztajn, L. M., Elliott, E. & Koren, O. The microbiota and the hypothalamus-pituitary-adrenocortical (HPA) axis, implications for anxiety and stress disorders. *Current Opinion in Neurobiology* **62**, 76–82 (2020).
7. Noguera, J. C., Aira, M., Pérez-Losada, M., Domínguez, J. & Velando, A. Glucocorticoids modulate gastrointestinal microbiome in a wild bird. *R. Soc. open sci.* **5**, 171743 (2018).
8. Brunetti, A. E. *et al.* Convergence of gut microbiota in myrmecophagous amphibians. *Proc. R. Soc. B.* **290**, 20232223 (2023).
9. Jiménez, R. R. & Sommer, S. The amphibian microbiome: natural range of variation, pathogenic dysbiosis, and role in conservation. *Biodivers Conserv* **26**, 763–786 (2017).
10. Bletz, M. C. *et al.* Amphibian gut microbiota shifts differentially in community structure but converges on habitat-specific predicted functions. *Nat Commun* **7**, 13699 (2016).
11. Kohl, K. D., Cary, T. L., Karasov, W. H. & Dearing, M. D. Restructuring of the amphibian gut microbiota through metamorphosis: The amphibian gut microbiota. *Environmental Microbiology Reports* **5**, 899–903 (2013).
12. Yang, L., Zhao, S. & Liu, S. A global analysis of urbanization effects on amphibian richness: Patterns and drivers. *Global Environmental Change* **73**, 102476 (2022).
13. Park, J.-K., Park, W.-B. & Do, Y. Tadpole growth rates and gut bacterial community: Dominance of developmental stages over temperature variations. *PLoS ONE* **18**, e0292521 (2023).
14. Knutie, S. A., Wilkinson, C. L., Kohl, K. D. & Rohr, J. R. Early-life disruption of amphibian microbiota decreases later-life resistance to parasites. *Nat Commun* **8**, 86 (2017).
15. Warne, R. W., Kirschman, L. & Zeglin, L. Manipulation of gut microbiota during critical developmental windows affects host physiological performance and disease susceptibility across ontogeny. *Journal of Animal Ecology* **88**, 845–856 (2019).

16. Billet, L. S., Hernández-Gómez, O. & Skelly, D. K. Ranavirus Epizootics and Gut Bacteriome Dysbiosis in Tadpoles: Evidence for the Anna Karenina Principle? *Molecular Ecology* **34**, e70022 (2025).
17. Crossland, M. R., Shine, R. & DeVore, J. L. Mechanisms, costs, and carry-over effects of cannibal-induced developmental plasticity in invasive cane toads. *Ecology and Evolution* **14**, e10961 (2024).
18. Denver, R. J. Environmental Stress as a Developmental Cue: Corticotropin-Releasing Hormone Is a Proximate Mediator of Adaptive Phenotypic Plasticity in Amphibian Metamorphosis. *Hormones and Behavior* **31**, 169–179 (1997).
19. Denver, R. J. Neuroendocrinology of Amphibian Metamorphosis. in *Current Topics in Developmental Biology* vol. 103 195–227 (Elsevier, 2013).
20. Assis, V. R., Robert, J. & Titon, S. C. M. Introduction to the special issue Amphibian immunity: stress, disease and ecoimmunology. *Phil. Trans. R. Soc. B* **378**, 20220117 (2023).
21. Petrullo, L. *et al.* Glucocorticoids coordinate changes in gut microbiome composition in wild North American red squirrels. *Sci Rep* **12**, 2605 (2022).
22. Bai, L. *et al.* Ecdysone-mediated intestinal growth contributes to microbiota-driven developmental plasticity under malnutrition. *Development* **153**, dev204909 (2026).
23. Gilbert, S. F., Bosch, T. C. G. & Ledón-Rettig, C. Eco-Evo-Devo: developmental symbiosis and developmental plasticity as evolutionary agents. *Nat Rev Genet* **16**, 611–622 (2015).
24. Gabor, C. R., Villatoro-Castañeda, M., Carlos-Shanley, C., Ujhegyi, N. & Bókony, V. Gut Bacterial Communities Vary across Habitats and Their Diversity Increases with Increasing Glucocorticoids in Toad Tadpoles. *Diversity* **15**, 23 (2022).
25. Rollins-Smith, L. A. & Le Sage, E. H. Heat stress and amphibian immunity in a time of climate change. *Phil. Trans. R. Soc. B* **378**, 20220132 (2023).
26. Miller, A. J. & Voyles, J. The impact of microbiome diversity and composition on host health and susceptibility to disease across amphibian life stages. *Front. Amphib. Reptile Sci.* **3**, 1666714 (2026).
27. Gould, T. J., Taylor, M. & Santelli, C. Aviti Sequencing and Marker Gene Data Analysis. Preprint at https://doi.org/10.64898/2026.02.06.704475 (2026).
28. Zhang, M. *et al.* The Changes in the Frog Gut Microbiome and Its Putative Oxygen-Related Phenotypes Accompanying the Development of Gastrointestinal Complexity and Dietary Shift. *Front. Microbiol.* **11**, 162 (2020).
29. Schreiber, A. M., Cai, L. & Brown, D. D. Remodeling of the intestine during metamorphosis of Xenopus laevis. *Proc Natl Acad Sci U S A* **102**, 3720–3725 (2005).
30. He, W. *et al.* Circadian Expression of Migratory Factors Establishes Lineage-Specific Signatures that Guide the Homing of Leukocyte Subsets to Tissues. *Immunity* **49**, 1175-1190.e7 (2018).
31. Scalvenzi, T., Clavereau, I., Bourge, M. & Pollet, N. Gut microbial ecology of Xenopus tadpoles across life stages. *Peer Community Journal* **1**, e41 (2021).
32. Stothart, M. R. *et al.* Stress and the microbiome: linking glucocorticoids to bacterial community dynamics in wild red squirrels. *Biol. Lett.* **12**, 20150875 (2016).
33. MacLeod, K. J., Kohl, K. D., Trevelline, B. K. & Langkilde, T. Context-dependent effects of glucocorticoids on the lizard gut microbiome. *Molecular Ecology* **31**, 185–196 (2022).
34. Sun, Z. *et al.* Bidirectional regulation of the brain-gut axis in *Macaca mulatta* : implications for wildlife conservation and experimentation. *Microbiol Spectr* **13**, e01338-25 (2025).

35. Song, X., Gao, L. & Wang, J. A promising bacterium-based strategy to control dengue transmission in mosquitoes. *Innovation (Camb)* **5**, 100708 (2024).
36. La Rosa, S. L. *et al.* Glycan processing in gut microbiomes. *Current Opinion in Microbiology* **67**, 102143 (2022).
37. Jeong, Y. S. *et al.* Gut microbiome shifts during frog development parallel host-association patterns across vertebrate lineages. *Front. Microbiol.* **17**, 1931668 (2026).
38. Sayols-Baixeras, S. *et al. Streptococcus* Species Abundance in the Gut Is Linked to Subclinical Coronary Atherosclerosis in 8973 Participants From the SCAPIS Cohort. *Circulation* **148**, 459–472 (2023).
39. Li, L. *et al.* The mediating effect of circulating inflammatory proteins on the relationship between gut microbiota and FD: a bidirectional Mendelian randomization study. *Sci Rep* **14**, 23785 (2024).
40. Chang, L. *et al.* The effects of corticosterone and background colour on tadpole physiological plasticity. *Comparative Biochemistry and Physiology Part D: Genomics and Proteomics* **39**, 100872 (2021).
41. Middlemis Maher, J., Werner, E. E. & Denver, R. J. Stress hormones mediate predator-induced phenotypic plasticity in amphibian tadpoles. *Proc. R. Soc. B.* **280**, 20123075 (2013).
42. Pereira, K. E., Bletz, M. C., McCartney, J. A., Woodhams, D. C. & Woodley, S. K. Effects of exogenous elevation of corticosterone on immunity and the skin microbiome of eastern newts (*Notophthalmus viridescens*). *Phil. Trans. R. Soc. B* **378**, 20220120 (2023).
43. Petranka, J. W. & Thomas, D. A. G. Explosive breeding reduces egg and tadpole cannibalism in the wood frog, Rana sylvatica. *Animal Behaviour* **50**, 731–739 (1995).
44. Skelly, D. K. Microgeographic countergradient variation in the wood frog, rana sylvatica. *Evolution* **58**, 160–165 (2004).
45. Beaupre, S. J., Jacobson, E. R., Lillywhite, H. B. & Zamudio, K. Guidelines for Use of Live Amphibians and Reptiles in Field and Laboratory Research. (2004).
46. Gosner, K. A simplified table for staging anuran embryos and larvae with notes on identification. *Herpetologica* **16**, 183–190 (1960).
47. Gomez-Mestre, I., Kulkarni, S. & Buchholz, D. R. Mechanisms and Consequences of Developmental Acceleration in Tadpoles Responding to Pond Drying. *PLoS ONE* **8**, e84266 (2013).
48. Gohl, D. *et al.* An optimized protocol for high-throughput amplicon-based microbiome profiling. *Protocol Exchange* https://doi.org/10.1038/protex.2016.030 (2016) doi:10.1038/protex.2016.030.
49. Andrews, S. FASTQC: A quality control tool for high throughput sequence data. Babraham Bioinformatics (2010).
50. Martin, M. Cutadapt removes adapter sequences from high-throughput sequencing reads. *EMBnet j.* **17**, 10 (2011).
51. Callahan, B. J. *et al.* DADA2: High-resolution sample inference from Illumina amplicon data. *Nat Methods* **13**, 581–583 (2016).
52. McLaren, M. R. Silva SSU taxonomic training data formatted for DADA2 (Silva version 138). Zenodo https://doi.org/10.5281/ZENODO.3731174 (2020).
53. Davis, N. M., Proctor, D. M., Holmes, S. P., Relman, D. A. & Callahan, B. J. Simple statistical identification and removal of contaminant sequences in marker-gene and metagenomics data. Preprint at https://doi.org/10.1101/221499 (2017).

54. Katoh, K. & Standley, D. M. MAFFT Multiple Sequence Alignment Software Version 7: Improvements in Performance and Usability. *Molecular Biology and Evolution* **30**, 772–780 (2013).
55. Piñeiro, C., Abuín, J. M. & Pichel, J. C. Very Fast Tree: speeding up the estimation of phylogenies for large alignments through parallelization and vectorization strategies. *Bioinformatics* **36**, 4658–4659 (2020).
56. Wood, S. N. Fast stable restricted maximum likelihood and marginal likelihood estimation of semiparametric generalized linear models. (2011).
57. Lahti, L. & Shetty, S. Microbiome R Pacakge. (2019).
58. Schliep, K. P. Phangorn: phylogenetic analysis in R. (2011).
59. Kembel, S. W. *et al.* Picante: R tools for integrating phylogenies and ecology. (2010).
60. Oksanen, J. *et al.* vegan: Community Ecology Package. 2.7-3 https://doi.org/10.32614/CRAN.package.vegan (2001).
61. Garcia Mendez, D. F., Egan, S., Wist, J., Holmes, E. & Sanabria, J. Meta-analysis of the Microbial Diversity Cultured in Bioreactors Simulating the Gut Microbiome. *Microb Ecol* **87**, 57 (2024).
62. Martinez, P. A. _pairwiseAdonis: Pairwise Multilevel Comparison using Adonis_. (2017).
63. Halekoh, U., Højsgaard, S. & Yan, J. The *R* Package **geepack** for Generalized Estimating Equations. *J. Stat. Soft.* **15**, (2006).
64. Glennemeier, K. A. & Denver, R. J. Developmental Changes in Interrenal Responsiveness in Anuran Amphibians. *Integrative and Comparative Biology* **42**, 565–573 (2002).
65. Mausbach, J., Laurila, A. & Räsänen, K. Context dependent variation in corticosterone and phenotypic divergence of Rana arvalis populations along an acidification gradient. *BMC Ecol Evo* **22**, 11 (2022).
66. McGillycuddy, M., Warton, D. I., Popovic, G. & Bolker, B. M. Parsimoniously Fitting Large Multivariate Random Effects in **glmmTMB**. *J. Stat. Soft.* **112**, (2025).
67. Douglas, G. M. *et al.* PICRUSt2 for prediction of metagenome functions. *Nat Biotechnol* **38**, 685–688 (2020).
68. Kanehisa, M., Sato, Y., Kawashima, M., Furumichi, M. & Tanabe, M. KEGG as a reference resource for gene and protein annotation. *Nucleic Acids Res* **44**, D457–D462 (2016).
69. Kanehisa, M. KEGG: Kyoto Encyclopedia of Genes and Genomes. *Nucleic Acids Research* **28**, 27–30 (2000).
70. Yu, G. Thirteen years of clusterProfiler. *The Innovation* **5**, 100722 (2024).

Acknowledgements

We thank Adriana Rubenstein, Dr. L. Kealoha Freidenburg, Lorenzo Tovanche and Carter Zelenitz for their assistance with logistics, field collection, and sample processing. We thank Dr. Logan Billet for his assistance with manuscript review. We also thank the Yale Reproductive Ecology Lab and specifically Dr. Gary Aronsen for use of hormone analysis equipment and assistance with laboratory methods and supervision. This project was supported by funding awarded to S.M.T from the Kohlberg-Donohoe Research Fellowship, and the Schiff Fund for Wildlife both subsidiaries from Yale University. Animal handling was approved by Yale University IACUC protocol # 2025-10361 and 2022-10361. Specimens were collected under CT DEEP Permit #2528001. Field surveys were conducted with permission from Yale Myers Research Committee (TRA24).

Author Contributions Statement

Samantha M. Tracy: writing - original draft, writing – review and editing, conceptualization, field collection, data curation, laboratory analysis, formal data analysis, funding acquisition, investigation, methodology, visualization. **David K. Skelly:** writing – review and editing, conceptualization, funding acquisition, resources, supervision.

Data Availability

Raw sequence data are available via the NCBI sequence Read Archive under Bioproject Accession Number PRJNA1493058. The datasets generated and analyzed in the current study are available in the DRYAD repository: http://datadryad.org/share/LINK_NOT_FOR_PUBLICATION/9_iOIMoSCzuY_Z8rJNqzdvocJFjXRw4JFm3qGBpY0dk

Additional Information

The authors declare no competing interests

Figure Legends

Figure 1: Map of study ponds in CT A) Ponds in the Yale Myers Forest with Forest property boundary B) Ponds in Madison, CT

Figure 2: Changes in alpha diversity metrics across the developmental window (A) Shannon Diversity Index (R^2= 0.240, $p < 0.001$) (B) Chao1 (R^2= 0.533, $p < 0.001$) (C) Faith's Phylogenetic Diversity (R^2= 0.528, $p < 0.001$). Trend lines and confidence intervals were generated by predicting alpha metrics using the stage term in the model. The p-value represents the p-value of the smoothed stage term in the GAM.

Figure 3: PCoA of three distance matrices clustered by stage category (A) Bray-Curtis (F = 6.26, $p = 0.001$) (B) Unweighted UniFrac (F = 3.86, $p = 0.001$) (C) Weighted UniFrac (F = 5.38, p =0.001). Axes represent the first two principal components of PCoA analysis with the amount of variation explained noted in parenthesis.

Figure 4: Shifts in the microbiome during development based on ASVs and Order. (A) Venn Diagram showing overlapping ASVs between various developmental stage categories. Circles correspond to distinct stage groupings; shading is consistent with the number of unique ASVs overlapping between circles and is consistent with the number and percent of total ASVs indicated inside the circle. (B) Stacked bar chart showing average relative abundance of orders across Gosner stages

Figure 5: Modeled relationships between average natural log baseline CORT and alpha diversity metrics (A) Shannon Diversity Index (ß = -0.138, $p = 0.153$) (B) Chao1 (ß = -235.8, $p = 0.003$) (C) Faith's Phylogenetic Diversity (ß = -18.27 $p = 0.03$). Trend lines were generated by predicting alpha metrics using the average baseline CORT term in the model. Beta values represent the beta coefficients of the CORT term in the GEE model and p-values are also specific to those model terms.

Figure 6: Effect estimates from negative binomial models showing the top 20 microbial genera associated with (A) developmental stage (BH adjusted p-value < 0.05) and (B) average baseline CORT when adjusting for stage (BH adjusted p-value < 0.05) . The x-axis shows modeled effect estimate sizes, the y-axis shows the names of microbial genera groups, the color shows the directionality of the effect estimate with blue bars indicating a positive association and red bars indicating a negative association.

Figure 7: Top NES estimates of functional KEGG Pathways associated with (A) developmental stage and (B) Baseline CORT (Top 20 by NES). Normalized Enrichment Score is shown on the x-axis, and the direction of association is color coded with negative associations with stage shown in red and positive associations shown in blue. The number of genes associated in that descriptive category are depicted by the size of the symbol.

Supplementary Files

This is a list of supplementary files associated with this preprint. Click to download.

- TableS8.csv
- TableS6.csv
- TableS5.csv
- TableS7.csv
- SupplementaryFigures.docx
- TableS4.csv
- SupplementaryTables1to3.docx